Gondwana Research 22 (2012) 799–809

Contents lists available at SciVerse ScienceDirect

Gondwana Research

journal homepage: www.elsevier.com/locate/gr

Granulites, CO_2 and graphite

Jan Marten Huizenga [a,*], Jacques L.R. Touret [b]

[a] Department of Geology, School of Environmental Sciences and Development, North-West University, Private Bag X6001, Potchefstroom, 2520, South Africa
[b] Musée de Minéralogie, MINES ParisTech, 75272 Paris Cedex 06, France

ARTICLE INFO

Article history:
Received 25 October 2011
Received in revised form 12 March 2012
Accepted 24 March 2012
Available online 30 March 2012

Handling Editor: M. Santosh

Keywords:
Graphite precipitation
CO2
C – O – H fluid
Granulite
Petrology
Tectonics

ABSTRACT

Externally derived, pure CO_2 that mixes with a carbon-(under)saturated C-O-H – fluid in lower crustal granulites may result in graphite precipitation if the host-rock oxygen fugacity ($f_{O_2}^{rock}$) is below the upper f_{O_2} limit of graphite. The maximum relative amount of graphite that can precipitate varies between a few mol% up to more than 25 mol%, depending on pressure, temperature, and host-rock redox state. The maximum relative amount of graphite that can precipitate from an infiltrating CO_2 fluid into a dry granulite (C – O fluid system) varies between zero and a few mol%. Thermodynamic evaluation of the graphite precipitation process shows that CO_2 infiltration into lower crustal rocks does not always result in a carbon (super)saturated fluid. In that case, graphite precipitation is only possible if carbon saturation can be reached as a result of the reaction $CO_2 \rightarrow CO + ½\ O_2$. Graphite that has been precipitated during granulite facies metamorphic conditions can subsequently be absorbed by a C – O – H fluid during retrograde metamorphism. It is also possible, however, that significant amounts of graphite precipitate from a C – O – H fluid during retrograde metamorphism. This study shows that interpreting the presence or absence of graphite in granulites with respect to CO_2 infiltration requires detailed information on the P–T–$f_{O_2}^{rock}$ conditions, the relative amount of CO_2 that infiltrates into the rock, and whether H_2O is present or not.

1. Introduction

The finding of CO_2 fluid inclusions in lower crustal rocks, first in southern Norway (Touret, 1971), then in granulites worldwide, has demonstrated the unambiguous relationship between CO_2 and high-grade metamorphism (e.g., Santosh and Omori, 2008). Initially, CO_2 was considered to be the only significant fluid in granulites but this idea was subsequently modified by including concentrated brines as an additional typical granulite fluid (e.g., Newton et al., 1998). Observations that support the idea of fluid-assisted granulite metamorphism (see Touret and Huizenga, 2011, 2012, for an overview) include the occurrence of fluid inclusions, field evidence (e.g., incipient charnockites, Santosh et al., 1990), and petrologic evidence such as intergranular metasomatic reactions (e.g., Touret and Nijland, 2012).

The debate on how CO_2 has been introduced into the rock system at granulite facies P–T conditions is still continuing (e.g., Touret and Huizenga, 2011). Internal CO_2 generation is a distinct possibility, which can be caused by, for example: (1) carbon oxidation in graphite-bearing sediments by H_2O derived from dehydration reactions (Touret, 1971) or crystallising granitic melts (Hollister, 1988), (2) Fe^{3+} reduction during partial melting in graphitic metapelites (Cesare et al., 2005), or (3) selective H_2O fractionation into a melt phase (Fyfe, 1973; Cesare and Maineri, 1999) during which the CO_2 content of the fluid phase increases and may even become carbon supersaturated resulting in graphite precipitation (e.g., Luque et al., 1998, 2012).

Alternatively, CO_2 can also be derived from an external source, in particular the mantle. The idea of mantle derived CO_2 infiltration into the lower crust was first proposed in 1980 by Newton et al. (1980), referred to as the "carbonic wave". This idea was opposed based on the fact that CO_2 is not able to migrate through lower crustal rock over large distances (Watson and Brenan, 1987). This argument, however, became less relevant when it was realised that CO_2 transportation occurred through mantle-derived magmas that are emplaced into the lower crust at granulite facies metamorphic conditions (e.g., Touret, 1992). Further, supporting evidence for a CO_2 mantle source has been obtained from the carbon isotopic signature of CO_2 in fluid inclusions (Jackson et al., 1988) and graphite (Farquhar and Chacko, 1991; Santosh and Wada, 1993a,b), and the helium isotope signature in fluid inclusions (e.g., Dunai and Touret, 1993). There is in our opinion convincing evidence from numerous granulite occurrences that CO_2 infiltration has occurred into the lower crust. This does, however, not necessarily mean that CO_2 was actively involved in the stabilisation of orthopyroxene and granulite genesis; CO_2 infiltration may have occurred in an already dry rock (e.g., Pili et al., 1998; Harley, 2004).

1.1. Graphite in granulites

Graphite occurs frequently in granulite facies metamorphic rocks (e.g., Santosh and Omori, 2008). In some cases the graphite content is so large that it has influenced the local name of the formation (Système du

* Corresponding author. Tel.: +27 18 299 2526; fax: +27 18 299 2370.
E-mail address: jan.huizenga@nwu.ac.za (J.M. Huizenga).

1342-937X/$ – see front matter
doi:10.1016/j.gr.2012.03.007

Graphite, Madagascar, e.g. Berglund and Touret, 1976; Collins et al., 2012). Peak metamorphic occurrences of graphite in ultrahigh temperature granulites ($T>1000$ °C) have, to our knowledge, not been reported. Large-scale hydrothermal graphite veins post dating granulite metamorphism are found in e.g., Sri-Lanka (e.g., Binu-Lal et al., 2003) and New Hampshire (Rumble et al., 1986).

Petrographical observations and carbon stable isotope data show that graphite in high-grade metamorphic rocks can be the result of different processes, notably: (1) prograde heating of pre-metamorphic organic matter in detrital rocks (e.g., Andreae, 1974; Rumble et al., 1977; Wada et al., 1995); (2) carbonate reduction in former calcareous rocks (Nockleberg, 1973; Perry and Ahmad, 1977), and (3) precipitation from a C–O–H fluid (i.e., epigenetic graphite) (e.g., Luque et al., 1998).

Examples of granulite facies epigenetic graphite include occurrences in granulite terrains in southern India (Santosh and Wada, 1993a,b; Radhika and Santosh, 1996; Farquhar et al., 1999; Santosh et al., 2003; Satish-Kumar et al., 2011) and the southern Iberian Massif (Rodas et al., 2000; Crespo et al., 2004). An example of high-temperature fluid precipitated graphite is shown in Fig. 1. Here, graphite occurs in the leucosomes of migmatites (Fig. 1), indicating that a carbon-saturated fluid either coexisted with or exsolved from a crystallising melt phase (Satish-Kumar et al., 2011). The migmatites are the result of fluid-present evolving towards fluid-absent partial melting at $T>850$ °C (Satish-Kumar et al., 2011).

It has been argued that granulite facies epigenetic graphite can be attributed to the infiltration of externally derived CO_2 fluid into a relatively reduced host-rock environment (Glassley, 1982; Lamb and Valley, 1984; Farquhar and Chacko, 1991; Santosh and Wada, 1993a,b; Radhika and Santosh, 1996; Binu-Lal et al., 2003; Santosh and Omori, 2008). As a result, the presence or absence of graphite in granulites has been used as an argument either supporting (e.g., Santosh and Omori, 2008) or opposing (Lamb and Valley, 1984) infiltration of externally derived CO_2 into lower crustal rocks, respectively. Thermodynamic calculations of the C–O–H fluid system for relevant P–T–f_{O_2} conditions demonstrate that any significant CO_2 infiltration should result in the precipitation of noticeable quantities of graphite if the host-rock has a f_{O_2} that allows graphite to occur as a stable phase (Glassley, 1982; Lamb and Valley, 1984, 1985).

The main purpose of this study is to probe whether the presence or absence of graphite in granulites can be used as an indication supporting or opposing CO_2 infiltration into lower crustal rocks. We will discuss the conditions under which graphite will precipitate when external CO_2 enters lower crustal rocks that either comprise a H_2O-bearing C–O–H fluid or are completely dry, using thermodynamic calculations. We will also discuss the effect that retrograde metamorphism has on the ability of a fluid to either precipitate or consume graphite.

Fig. 1. Elongated graphite crystals along feldspar grain boundaries in a leucosome from a migmatite (sample KKB-21-1-B, see Fig. 1 in Satish-Kumar et al., 2011) in the Kerela Khondalite Belt in southern India (Satish-Kumar et al., 2011). Base of the photograph corresponds to 14 mm. Photo courtesy Bernardo Cesare (University of Padova, Italy).

2. CO_2 infiltration into H_2O-bearing lower continental crust: C–O–H fluid system

2.1. Introduction

We will illustrate thermodynamic calculations in the graphite–C–O–H system by using isobaric-isothermal C–O–H ternary diagrams (e.g., Huizenga, 2011). These diagrams are perfectly suitable to illustrate what happens when CO_2 infiltrates into a relatively reduced environment. Fluid composition calculations in the C–O–H system are explained in numerous papers (e.g., French, 1966; Ohmoto and Kerrick, 1977; Huizenga, 2001, and references therein) and not repeated here. Thermodynamic data for the fluid species and graphite for calculating equilibrium constants for the independent reactions between the different fluid species were taken from Holland and Powell (1998). Fugacity coefficients for the fluid species were calculated as described by Shi and Saxena (1992) assuming ideal mixing. The use of a different method such as described by Zhang and Duan (2010) results only in very small concentration differences of the dominant fluid species for the P–T range of interest (1–15 kbar, 400–1100 °C). All calculations were carried out using an updated version of the COH Excel spreadsheet (Huizenga, 2005).

The Fayalite–Magnetite–Quartz buffer (FMQ) is used as a reference for the oxygen fugacity, which is calculated from the equation given by Ohmoto and Kerrick (1977): $\log_{10} f_{O_2}^{FMQ} = -25738/T_{kelvin} + 9.00 + 0.092\ (P_{atm.}-1)/T_{kelvin}$. The choice of using FMQ as a reference f_{O_2} buffer is justified by the fact that high-grade metamorphic rocks have typically oxygen fugacities around the FMQ buffer (Bohlen and Essene, 1977; Lamb and Valley, 1985; Skippen and Marshall, 1991; Harlov, 1992, 2000; Török et al., 2005). In this study, we have restricted our modelling to $\log_{10} f_{O_2} > FMQ-2$; granulites that are more reduced have, to our knowledge, not been reported so far.

The composition of a carbon-saturated fluid, i.e. a fluid of which the carbon activity (a_C^{fluid}) is 1 (i.e., graphite present), varies with the oxygen fugacity of the fluid phase ($f_{O_2}^{fluid}$). These carbon-saturated fluids are situated on the carbon saturation surface (Fig. 2a). The position of the carbon saturation surface shifts with changing P and T, i.e. it moves closer to the C-apex with isothermal decompression whereas it does the opposite with isobaric cooling (e.g., Luque et al., 1998). Fluids that have compositions above the carbon saturation surface (grey field in Fig. 2a) are supersaturated in carbon ($a_C^{fluid}>1$), i.e. these fluids will precipitate graphite. On the other hand, fluids that have compositions below the carbon saturation surface are undersaturated with respect to carbon ($a_C^{fluid}<1$). Therefore, these fluids have the ability to consume graphite if present.

Oxidised carbon-saturated fluids (atomic $O/(O+H)$ or $X_O > ⅓$) comprise H_2O, CO_2, and CO whereas reduced carbon-saturated fluids ($X_O < ⅓$) consist of H_2O, CH_4, and H_2 (Fig. 2b). The f_{O_2} range for a H_2O-CO_2 ($\pm$CO) dominated carbon-saturated fluid is much smaller compared to the f_{O_2} range for a H_2O-CH_4 ($\pm H_2$) carbon-saturated fluid (Fig. 2a) (e.g., Ohmoto and Kerrick, 1977). Graphite is absent ($a_C^{fluid}<1$) if f_{O_2} exceeds the upper f_{O_2} limit for graphite to exist as a stable phase ($\log_{10} f_{O_2} > FMQ-0.60$ for $P=8$ kbar and $T=900$ °C, see Fig. 2a). Carbon-saturated fluids are almost pure CO_2 when X_O approaches 1 ($X_O \rightarrow 1$) at $T<\sim$700–800 °C. However, at $T > \sim$700–800 °C, carbon-saturated fluids of which $X_O \rightarrow 1$ do contain significant amounts of CO (Fig. 2c,d), i.e. the carbon saturation surface intersects the C-O binary above CO_2 (Fig. 2c), which implies that a pure CO_2 fluid is carbon undersaturated. Consequently, the mole fraction of CO in a C–O–H fluid of which $X_O \rightarrow 1$ is an indication for the degree of carbon undersaturation for a pure CO_2 fluid (Fig. 2c,d).

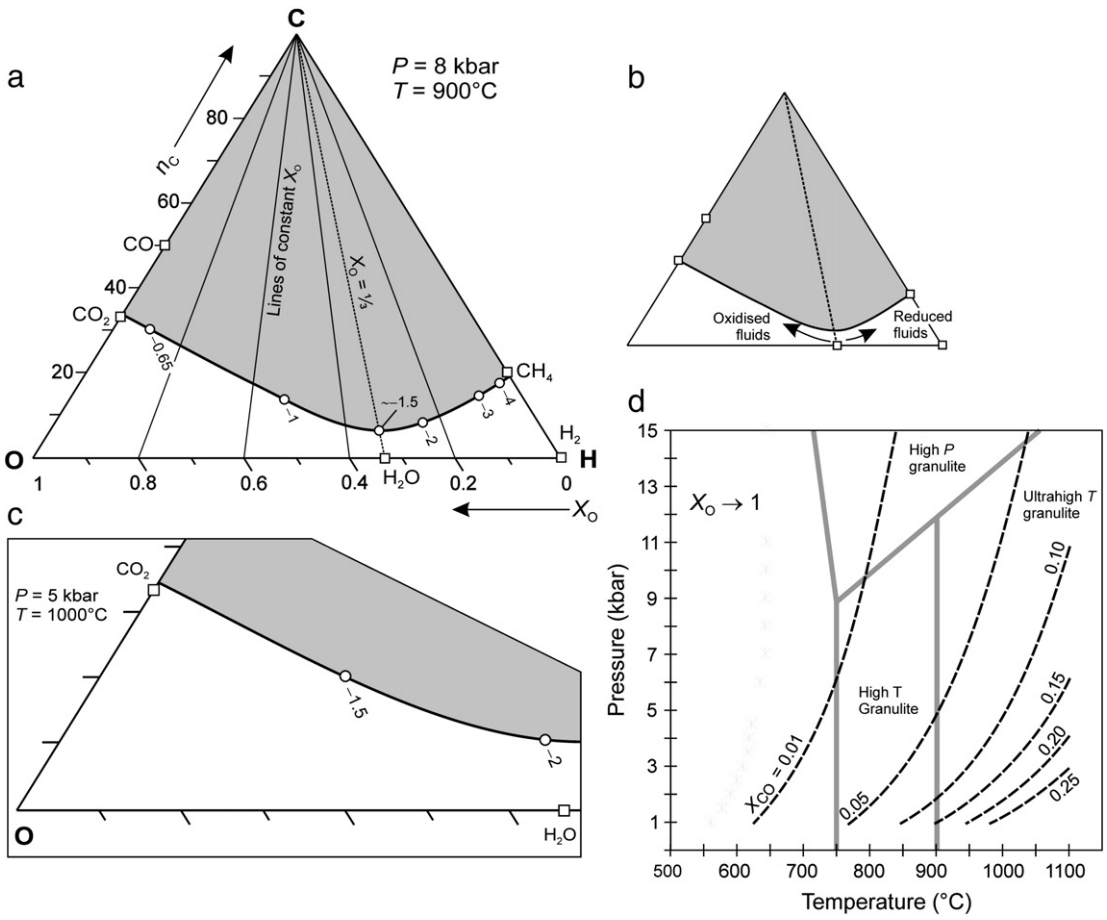

Fig. 2. (a) Isobaric-isothermal ($P=8$ kbar, $T=900$ °C) ternary C–O–H diagram illustrating the compositional variation of a carbon-saturated fluid (solid line) with changing $f_{O_2}^{fluid}$ (open circles, indicated relative to FMQ in $\log_{10}$ units). Grey area: field of carbon supersaturation. X_O: fluid O/(O + H) atomic ratio, n_C: fluid atomic carbon content, labelled in mol%. A C–O–H fluid with $X_O=⅓$ has a $\log_{10} f_{O_2}^{fluid}$ of ~FMQ − 1.5. (b) Indication of reduced ($X_O<⅓$) and oxidised ($X_O>⅓$) carbon-saturated C–O–H fluid, dominated by CO_2-$H_2O \pm CO$ and $CH_4-H_2O \pm H_2$, respectively. (c) Illustration of the position of the carbon saturation surface situated above CO_2 on the C–O binary ($P=5$ kbar, $T=1000$ °C) due to the presence of CO implying that pure CO_2 is carbon undersaturated. (d) Pressure–temperature diagram showing isopleths of the CO mole fraction (X_{CO}^{fluid}, dashed lines) for fluids of which $X_O \rightarrow 1$ (i.e., fluid that can coexists with graphite at its maximum $f_{O_2}^{fluid}$). For such a fluid, X_{CO}^{fluid} is an indication of the degree of carbon undersaturation surface for a pure CO_2 fluid. Granulite subfacies fields after Brown (2007).

2.2. CO_2 infiltration and graphite precipitation in the C–O–H system

The initial phase of isobaric–isothermal CO_2 infiltration involves the mixing of a carbon-undersaturated granulite C–O–H fluid with externally derived CO_2 during which the fluid mixture becomes enriched in CO_2 and subsequently approaches carbon saturation (stage 1 in Fig. 3, e.g., Lamb and Valley, 1984, 1985). Any further externally derived CO_2 that enters the system will subsequently mix with the carbon-saturated C–O–H fluid (stage 2 in Fig. 3), which results in graphite precipitation as the relatively oxidised (CO_2-rich) mixed fluid is reduced until fluid–rock redox equilibrium is achieved. This paper will focus solely on the second stage of the CO_2 infiltration process. For clarity, we will refer to the infiltrating CO_2 as the external fluid and the carbon-saturated fluid (present as an intergranular fluid in the granulite) as the internal fluid. Mixing of the external CO_2 and the internal carbon-saturated C–O–H fluid (stage 2, Fig. 3) may result in different graphite precipitation scenarios, which will be explained in the next sections using an example of CO_2 infiltrating a host-rock ($\log_{10} f_{O_2}^{rock} = FMQ-2$) at 5 kbar and 1000 °C (Fig. 4a–d).

2.2.1. Mixing of external and internal fluid: carbon-undersaturated fluid

Mixing of externally-derived CO_2 and the internal carbon-saturated C–O–H fluid can result in a relatively oxidised carbon-undersaturated fluid if the external–internal fluid ratio is relatively large. In this case, the composition of the mixed fluid is situated below the carbon saturation surface (Fig. 4b,c), which is caused by the fact that CO_2 is situated below the carbon saturation surface for the given P–T conditions (Fig. 4b,c). Therefore, the fluid will firstly adjust to the relatively reduced environment by its reduction to produce CO according to the net reaction:

$$CO_2 \rightarrow CO + ½\,O_2 (\text{to rock}) \quad (1)$$

where the released O_2 is absorbed by the host-rock (i.e., oxygen sink). As a consequence, the fluid composition becomes more reduced and moves towards the carbon saturation surface (path 1a in Fig. 4c). The fluid becomes carbon saturated ($a_c^{fluid}=1$) as soon as it reaches the carbon saturation surface. At this stage there are two scenarios as how to fluid re-equilibration may continue. The first one is that the above reaction will stop and the CO_2 (+CO) fluid will start precipitating graphite according to the net reactions (path 1b in Fig. 4c):

$$CO_2 \rightarrow C + O_2 (\text{to rock}) \quad (2)$$

and (to a lesser extent)

$$CO \rightarrow C + ½\,O_2 (\text{to rock}) \quad (3)$$

in which the fluid becomes more reduced as it approaches $f_{O_2}^{rock}$. In this case the fluid composition will change along the carbon saturation surface (path 1b in Fig. 4c) while the reaction proceeds until $\log_{10} f_{O_2}^{fluid} = \log_{10} f_{O_2}^{rock} = FMQ-2$. In this scenario, the driving force for re-equilibration is the redox difference between the fluid phase

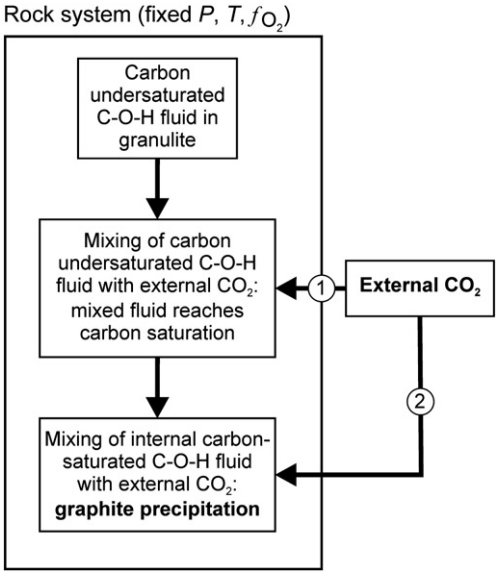

Fig. 3. Diagram illustrating the different stages of isobaric-isothermal external CO_2 infiltration into granulites. The initial stage (1) includes mixing of externally derived CO_2 (referred to as external fluid in the text) with the carbon-undersaturated fluid present in the host rock causing the mixed fluid to reach carbon saturation. Continuous CO_2 infiltration (stage 2) will result in mixing of CO_2 and the carbon-saturated fluid (referred to as internal fluid in the text). The resulting fluid mixture will either be carbon under- or supersaturated depending on the mixing ratio. Note that stage 1 becomes irrelevant if CO_2 infiltration occurs in lower crustal rocks that already comprise (biogenic) graphite.

and the host-rock ($f_{O_2}^{fluid} > f_{O_2}^{rock}$), i.e. graphite precipitation occurs under carbon-saturated conditions ($a_C^{fluid} = 1$).

The second option is that the CO_2 fluid continues its reduction without graphite precipitation (reaction 1) until it reaches fluid–rock redox equilibrium ($\log_{10} f_{O_2}^{fluid} = \log_{10} f_{O_2}^{rock} = FMQ-2$) (path 2a in Fig. 4c) during which it becomes carbon supersaturated. Consequently, graphite precipitation occurs (while a_C^{fluid} is decreasing) according to reactions 2 and 3 while $f_{O_2}^{fluid}$ remains constant until the fluid reaches its equilibrium composition on the carbon saturation surface (i.e., $a_c^{fluid} = 1$) (path 2b in Fig. 4c). In this case, the driving force for re-equilibration is the carbon-supersaturated state of the fluid phase.

2.2.2. Mixing of external and internal fluid: carbon-supersaturated fluid

Here, the mixed fluid is carbon supersaturated as its composition is somewhere on the mixing line that is situated above the carbon saturation surface (Fig. 4b,d). The re-equilibration process will firstly involve the reduction of the mixed fluid without graphite precipitation (reaction 1) until it reaches fluid–rock redox equilibrium ($\log_{10} f_{O_2} = FMQ-2$) (path 3a in Fig. 4d). This is followed by graphite precipitation (while a_C^{fluid} is decreasing) at constant $f_{O_2}^{fluid}$ ($= f_{O_2}^{rock}$) according to reactions 2 and 3 (path 3b in Fig. 4d).

2.2.3. How much graphite can precipitate?

The relative amount of graphite that can precipitate at isobaric–isothermal conditions depends on $f_{O_2}^{rock}$ and the external–internal fluid ratio. It can be determined by taking the difference between the atomic carbon content (n_C in mol%) of the external–internal fluid mixture and that of the internal carbon-saturated fluid (Δn_C, Fig. 5a). However, n_C of the external–internal fluid mixture is variable as it depends on the mixing ratio. Nevertheless, the maximum relative

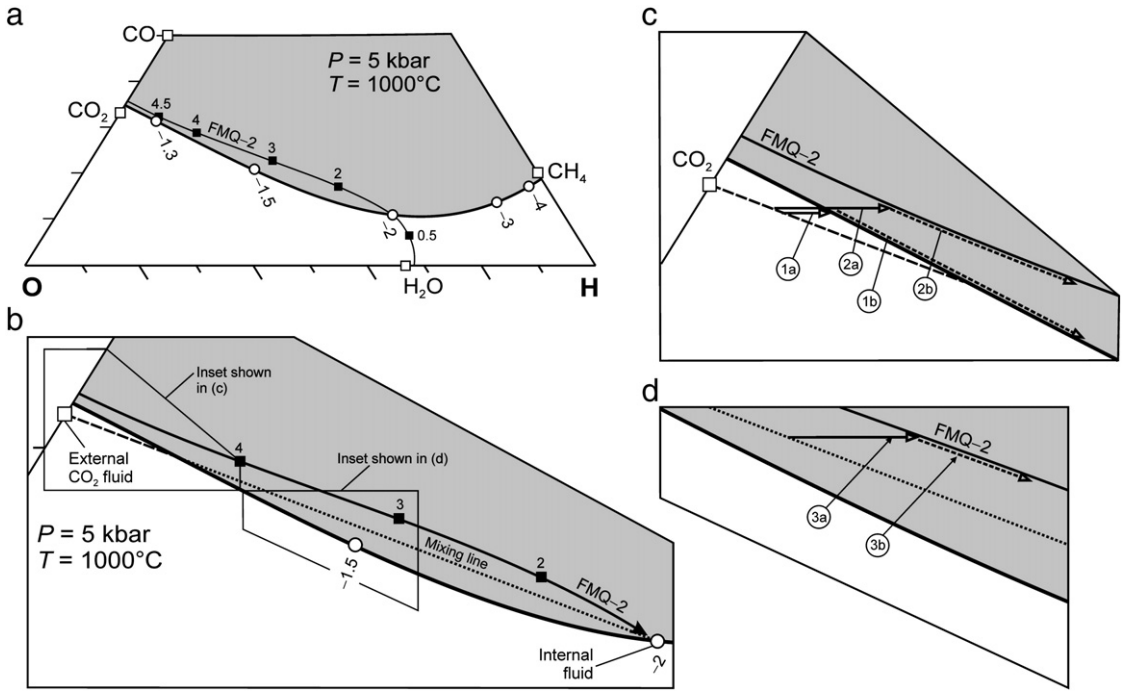

Fig. 4. (a) Bottom part of an isobaric-isothermal ($P = 5$ kbar, $T = 1000$ °C) ternary C–O–H diagram showing the compositional variation of a carbon-saturated fluid (thick line) with variable $f_{O_2}^{fluid}$ relative to FMQ (open circles, labelled in $\log_{10}$ units). Thin solid line: variation of fluid composition at $\log_{10} f_{O_2}^{fluid} = FMQ-2$ as a function of a_C^{fluid} (black squares). (b) Bottom part of a C–O–H diagram showing the mixing line between CO_2 and a carbon-saturated C–O–H fluid within a host rock with $\log_{10} f_{O_2}^{rock} = FMQ-2$ at $P = 5$ kbar and $T = 1000$ °C. Insets are enlarged in (c) and (d). Mixing of external CO_2 with an internal carbon-saturated C–O–H fluid will result in either a carbon under- or supersaturated fluid (dashed or dotted mixing line, respectively) depending on the mixing ratio. (c) Illustration of graphite precipitation from a carbon-undersaturated fluid. This fluid requires CO_2 reduction (reaction 1) in order to get carbon-saturated (path 1a). Graphite precipitation occurs as soon as the reduction of CO_2 has resulted in a carbon-saturated CO_2–CO fluid. Graphite precipitation from this fluid will proceed at conditions of carbon saturation while $f_{O_2}^{fluid}$ decreases until $f_{O_2}^{fluid} = f_{O_2}^{rock}$ (path 1b). Alternative, CO_2 reduction continues until $f_{O_2}^{fluid} = f_{O_2}^{rock}$ (path 2a). Consequently, this CO_2–CO fluid will be carbon supersaturated and subsequent graphite precipitation occurs at constant $f_{O_2}^{fluid}$ at decreasing a_C^{fluid} (path 2b). (d) Illustration of graphite precipitation from a carbon-supersaturated fluid. CO_2 will first reduce without graphite precipitation until $f_{O_2}^{fluid} = f_{O_2}^{rock}$ (n_C of the fluid remains constant, path 3a), after which graphite precipitation will occur while $f_{O_2}^{fluid}$ remains constant, i.e. (path 3b).

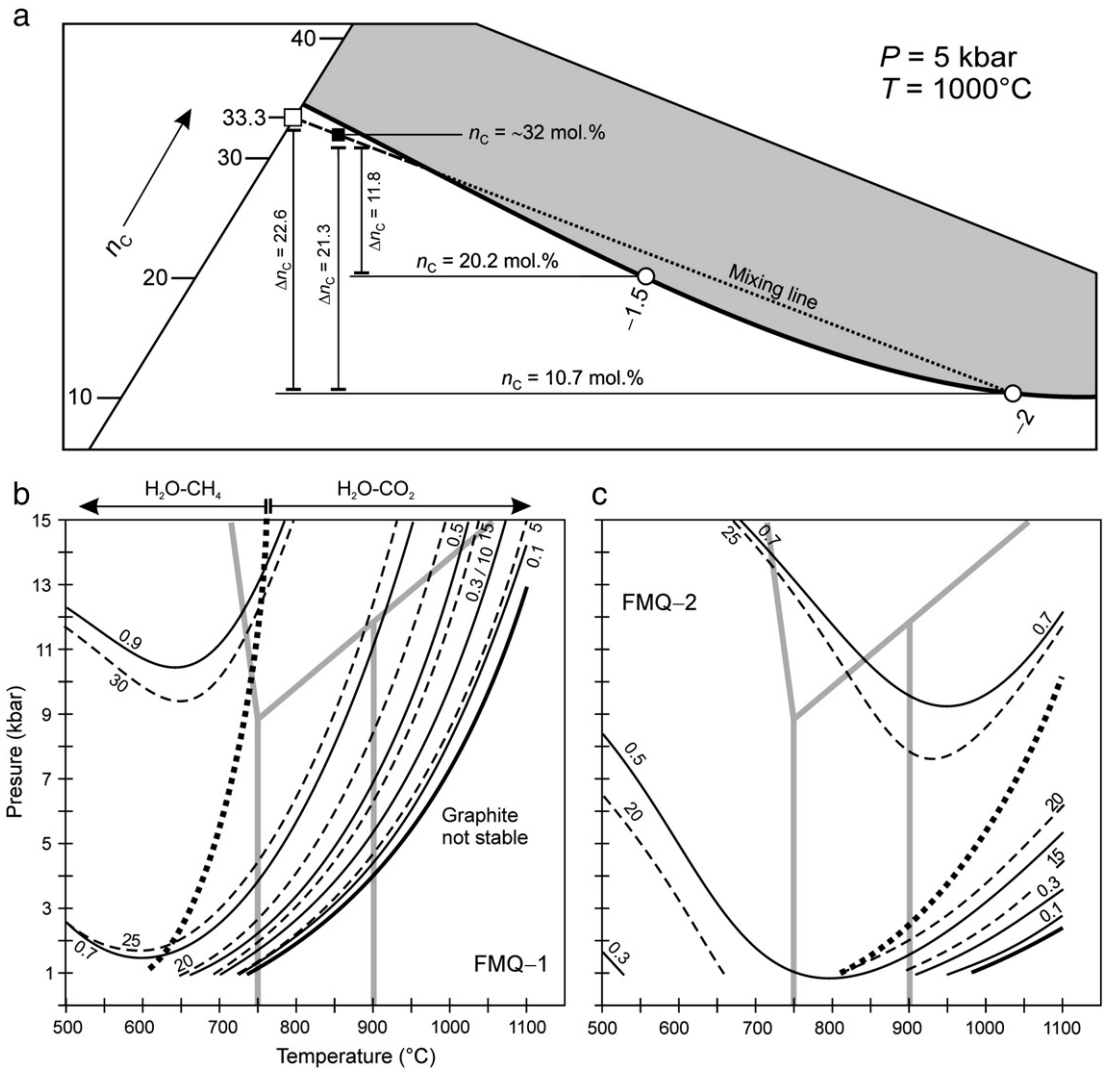

Fig. 5. (a) Determination of the relative amount of graphite that can precipitate from an external–internal fluid mixture (black square) for $\log_{10} f_{O_2}^{rock}$ = FMQ − 2 and FMQ − 1.5. For FMQ − 2, the relative amount of graphite that precipitates (Δn_C) is 21.3 mol% (32 minus 10.7), for FMQ − 1.5, this amount is 11.8 mol% (32 minus 20.2). The maximum relative amount of graphite that can precipitate is 22.6 mol% for FMQ − 2 (33.3 minus 10.7). See text for further discussion. (b) Pressure–temperature diagram showing (1) the mole fraction of H_2O (thin solid lines) of a carbon-saturated C–O–H fluid ($\log_{10} f_{O_2}^{fluid}$ = FMQ − 1), and (2) the maximum relative amount of graphite than can precipitate when CO_2 infiltrates a rock with $\log_{10} f_{O_2}^{rock}$ = FMQ − 1 (dashed lines, labelled in mol%). Dotted line: separation between fluids comprising H_2O and CH_4 (X_O < ⅓, low T), and H_2O and CO_2 (X_O > ⅓, high T). (c) Same as (b) but now for $\log_{10} f_{O_2}$ = FMQ − 2. Note that for both (b) and (c), the mole fraction of H_2O correlates positively with the maximum relative amount of graphite that can precipitate. Granulite subfacies indicated in (b) and (c) are after Brown (2007) (see Fig. 2d for field definitions).

amount of graphite that can precipitate can be determined if it is assumed that the external–internal fluid mixture has a n_C value corresponding to that of pure CO_2 (n_C = 33.3 mol%). This approximation is valid when the amount of external CO_2 that infiltrates is relatively large compared to the internal granulite fluid. The maximum relative amount of graphite that can precipitate shows a positive correlation with the H_2O mole fraction of the carbon-saturated fluid phase and varies with P, T, and $f_{O_2}^{rock}$ (Fig. 5b,c). The absolute amount of graphite that precipitates depends on the relative amount and the quantity of CO_2 fluid that infiltrates into the rock.

2.3. C – O – H fluid system: conclusions

The following can be concluded on graphite precipitation as a result of CO_2 infiltration into rocks at granulite facies P–T conditions:

(1) Graphite precipitation associated with CO_2 infiltration is only possible for host-rock redox conditions with maximum $\log_{10} f_{O_2}^{rock}$ values varying between ~FMQ + 0.2 and ~FMQ − 2.0 depending on the granulite facies P–T conditions (Fig. 6). In

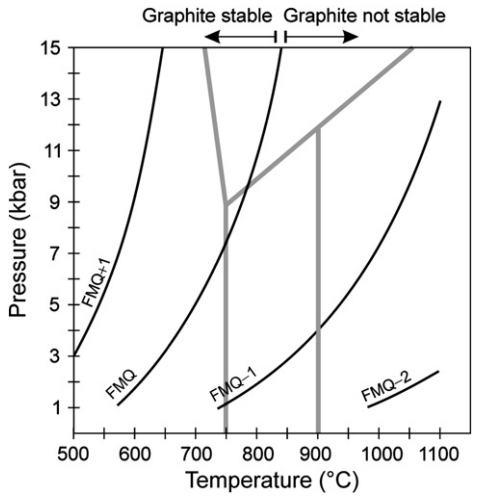

Fig. 6. Pressure–temperature diagram showing the graphite + C – O – H fluid stability field as a function of different oxygen fugacities (black lines, indicated as $\log_{10}$ values relative to FMQ). Granulite subfacies are after Brown (2007) (see Fig. 2d for field definitions).

a too oxidising environment, graphite cannot coexist with a C–O–H fluid.

(2) Mixing of an externally derived CO_2 with an internal carbon-saturated C–O–H fluid may result in either a mixed carbon-undersaturated or carbon-supersaturated fluid at granulite facies *P–T* conditions. Carbon-undersaturated fluids reach carbon (super)saturation if some CO_2 is reduced to CO (reaction 1), which is then followed by graphite precipitation according to reactions 2 and 3 (Fig. 4b–d).

(3) Carbon saturation and fluid–rock redox equilibrium cannot coexist simultaneously during graphite precipitation. The C–O–H fluid will either be in a state of (i) $a_C^{fluid} > 1$ and $f_{O_2}^{fluid} = f_{O_2}^{rock}$ or (ii) $a_C^{fluid} = 1$ and $f_{O_2}^{fluid} > f_{O_2}^{rock}$ until graphite precipitation is completed at which $a_C^{fluid} = 1$ and $f_{O_2}^{fluid} = f_{O_2}^{rock}$. Which one of these two scenarios occurs depends on the ability of graphite to nucleate as soon as carbon saturation is reached.

(4) The maximum relative amount of graphite that can precipitate shows a positive correlation with the mole fraction of H_2O in the carbon-saturated fluid phase. The absolute amount of graphite that precipitates depends on the quantity of CO_2 fluid that infiltrates into the rock.

3. CO_2 infiltration into H_2O-absent lower continental crust: C–O fluid system

Most granulites do show some evidence for the presence of H_2O as hydrous mineral phases like biotite or amphibole are present, even at peak metamorphic conditions. The absence of H_2O-bearing mineral phases in ultra-high temperature granulites (e.g., Berg, 1977; Hacker et al., 2000; Sajeev et al., 2007; Nasipuri et al., 2009; Zhang et al., 2011) indicates that these rocks were formed in an almost completely H_2O-absent environment. It is in this respect not a coincidence that that the most typical (ultra)high-density pure CO_2 fluid inclusions have been found in ultrahigh temperature minerals such as sapphirine (coexisting with quartz) and Al_2O_3-rich orthopyroxene (Tsunogae et al., 2002; Santosh et al., 2004, 2008). Completely dry conditions most likely also prevail at the onset of retrograde metamorphism when the rocks are still at relatively high temperatures. Any H_2O that enters the system during cooling, will be completely consumed by relatively fast non-equilibrium retrograde hydration reactions (e.g., Yardley, 1997, 2009). In both cases, i.e. CO_2 infiltration into ultrahigh temperature or cooling granulites, the C–O fluid system is thus applicable.

3.1. C–O fluid system calculations

Fluid species within the C–O system comprise CO, CO_2 and O_2, which are related by two independent reactions (Table 1). At a fixed *P* and *T*, a C–O fluid system is univariant, i.e. one variable of the possible four (a_C^{fluid}, $f_{O_2}^{fluid}$, mole fractions of CO_2 and CO in the fluid phase) must be fixed in order to calculate the others (Table 2, Fig. 7a–c). The relevant equations that are used for the calculations are shown in Table 2. Fig. 7a–c shows the calculation results for a C–O fluid system while fixing a_C^{fluid} (Fig. 7a), $f_{O_2}^{fluid}$ (Fig. 7b), or the CO_2 mole fraction in the fluid phase ($X_{CO_2}^{fluid}$) (Fig. 7c). Calculations show that for a pure CO_2 fluid ($X_{CO_2}^{fluid} = 0.999$), a_C^{fluid} will always be <1 at $T > \sim 500$–600 °C (Fig. 7c).

Table 1
Independent equilibrium reactions in the C–O fluid system.

Equilibrium reaction	Equilibrium constant
$CO + ½O_2 = CO_2$	$K_1 = f_{CO_2}/[f_{CO}(f_{O_2}^{fluid})^{½}] = \gamma_{CO_2} X_{CO_2}^{fluid}/[\gamma_{CO} X_{CO}^{fluid} (f_{O_2}^{fluid})^{½}]$
$C + O_2 = CO_2$	$K_2 = f_{CO_2}/(f_{O_2}^{fluid} a_C^{fluid}) = \gamma_{CO_2} X_{CO_2}^{fluid} P/(f_{O_2}^{fluid} a_C^{fluid})$

f_i, and γ_i denote the fugacity and fugacity coefficient of fluid species *i*, respectively, and are related to each other by the relation $f_i = \gamma_i X_i^{fluid} P$ (ideal mixing) (e.g., Huizenga, 2001). X_i^{fluid}: mole fraction of species *i* in the fluid phase.

However, similar to the C–O–H fluid system, this does not imply that graphite will not precipitate when CO_2 enters a rock at $T > 600$ °C. A CO_2 fluid will have relatively high $f_{O_2}^{fluid}$ (see example in Fig. 7c), i.e. if CO_2 infiltrates into a relatively reduced environment (i.e., $f_{O_2}^{fluid} > f_{O_2}^{rock}$) at isobaric and isothermal conditions, it will adapt by the reduction of CO_2 according to reaction 1 during which the carbon activity will increase.

This can be best illustrated with an example; suppose a pure CO_2 ($X_{CO_2}^{fluid} = 0.999$) infiltrates into a rock at a *P*, *T* and $\log_{10} f_{O_2}^{rock}$ of 11 kbar, 1000 °C, and FMQ − 1, respectively. Under the given *P* and *T* conditions, the CO_2 fluid will have a $\log_{10} f_{O_2}^{fluid}$ of FMQ + 2.7 and a a_C^{fluid} of 0.0003 (open square in Fig. 7c). Under these conditions, the CO_2 fluid will adapt to the reducing host-rock conditions, without any graphite precipitation, according to reaction 1. As this reaction proceeds, $f_{O_2}^{fluid}$ will decrease (approaching $f_{O_2}^{rock}$) while a_C^{fluid} will increase. Fluid carbon saturation is reached when $\log_{10} f_{O_2}^{fluid}$ of FMQ − 0.78 (stage 1 in Fig. 8a) i.e., still in redox disequilibrium with the host-rock. Further decrease of $f_{O_2}^{fluid}$ will result in the fluid to become carbon supersaturated; when fluid–rock redox equilibrium has been achieved at FMQ − 1, a_C^{fluid} will be 1.6 (stage 2 in Fig. 8a). At this point, graphite precipitation (stage 3 in Fig. 8b) may occur according to the net reaction:

$$2\,CO \rightarrow C + CO_2 \quad (4)$$

which causes $f_{O_2}^{fluid}$ to increase. In other words, graphite precipitation is only possible if $f_{O_2}^{fluid}$ can deviate from $f_{O_2}^{rock}$ (arbitrarily chosen as + 0.05 $\log_{10}$ unit in Fig. 8b). The relative amount of graphite that can precipitate is variable and depends on the amount that $f_{O_2}^{fluid}$ can increase relative to $f_{O_2}^{rock}$. However, $\log_{10} f_{O_2}^{fluid}$ can never exceed that of the carbon-saturated fluid at the specified *P–T* conditions: FMQ − 0.78. Consequently, the maximum relative amount of graphite that can precipitate is defined by the difference between the carbon content of the carbon-supersaturated fluid ($a_C^{fluid} = 1.6$, $n_C = 34.10$ mol%, Fig. 8b) and the carbon content of the carbon-saturated fluid ($n_C = 33.94$ mol%, Fig. 8a), i.e. 0.16 mol%. This maximum amount increases with decreasing $f_{O_2}^{rock}$, e.g. for a host-rock with $\log_{10} f_{O_2}^{fluid}$ of FMQ − 2, the maximum amount of graphite that can precipitate increases tenfold to ~1.6 mol% (Fig. 8c), but is still very small.

This example illustrates that, in contrast to the graphite–C–O–H fluid system, the graphite–C–O fluid system can never reach a condition in which $a_C^{fluid} = 1$ and $f_{O_2}^{fluid} = f_{O_2}^{rock}$. Consequently, a graphite–C–O fluid system will always be in a state of either $a_C^{fluid} > 1$ and $f_{O_2}^{fluid} = f_{O_2}^{rock}$, or $a_C^{fluid} = 1$ and $f_{O_2}^{fluid} > f_{O_2}^{rock}$. Furthermore, if $f_{O_2}^{rock}$ is greater than that of a carbon-saturated C–O fluid at the given *P-T* conditions (in the given example, $\log_{10} f_{O_2}^{rock} >$ FMQ − 0.78, see Fig. 8c), a C–O fluid cannot reach carbon saturation, i.e. graphite precipitation associated with CO_2 infiltration is impossible under these conditions.

3.2. C–O fluid system: conclusions

Generally, we can conclude the following about graphite precipitation from C–O fluids at granulite-facies conditions: (1) Pure CO_2 is undersaturated with respect to carbon and needs to be reduced to CO, according to reaction 1, in order to become carbon (super)saturated. (2) The relative amount of graphite that can precipitate from C–O fluids cannot be determined exactly as it depends on how much $f_{O_2}^{fluid}$ can deviate from $f_{O_2}^{rock}$. Graphite cannot precipitate if the fluid and rock are in redox equilibrium. However, if graphite does precipitate, then the maximum relative amount of graphite that can be formed depends on *P*, *T*, and $f_{O_2}^{rock}$ (Figs. 8c, 9a,b) and is in the order of a few mol.%, i.e. generally much smaller compared to the maximum amount of graphite that can precipitate from C–O–H fluids. Due to the small molar volume of graphite (~5.3 cm^3/mol), it is likely that any graphite that precipitates will not be noticed in a rock specimen. (3) $f_{O_2}^{rock}$ must be lower than $f_{O_2}^{fluid}$ of a carbon-saturated C–O fluid at given *P–T* conditions in order for any graphite to precipitate from CO_2. Infiltration of CO_2 can, therefore, only result in graphite precipitation if the maximum values of $\log_{10} f_{O_2}^{rock}$ vary

Table 2
Possible solutions within the C–O fluid system.

Variables known	Variables to be solved	Solutions
P, T, a_C^{fluid}	$f_{O_2}^{fluid}$, $X_{CO_2}^{fluid}$, X_{CO}^{fluid}	$f_{O_2}^{fluid} = \gamma_{CO_2}([4K_1^2P\,\gamma_{CO}^2 + K_2\,a_C^{fluid}\gamma_{CO_2}]^{½} - [K_2 a_C^{fluid}\gamma_{CO_2}]^{½})^2/(4a_C^{fluid}K_2K_1^2\gamma_{CO}^2)$ $X_{CO_2}^{fluid} = ([4K_1^2P\,\gamma_{CO}^2 + K_2\,a_C^{fluid}\gamma_{CO_2}]^{½} - [K_2 a_C^{fluid}\gamma_{CO_2}]^{½})^2/(4\,K_1^2P\,\gamma_{CO}^2)$ $X_{CO}^{fluid} = 1 - X_{CO_2}^{fluid}$
P, T, $f_{O_2}^{fluid}$	a_C^{fluid}, $X_{CO_2}^{fluid}$, X_{CO}^{fluid}	$a_C^{fluid} = K_1\,P\,\gamma_{CO_2}\gamma_{CO}/(K_2\,(f_{O_2}^{fluid})^{½}[K_1\,(f_{O_2}^{fluid})^{½}\gamma_{CO} + \gamma_{CO_2}])$ $X_{CO_2}^{fluid} = K_1\,(f_{O_2}^{fluid})^{½}\gamma_{CO}/(K_1\,(f_{O_2}^{fluid})^{½}\gamma_{CO} + \gamma_{CO_2})$ $X_{CO}^{fluid} = 1 - X_{CO_2}^{fluid}$
P, T, $X_{CO_2}^{fluid}$	$f_{O_2}^{fluid}$, $a_C^{fluid}X_{CO}^{fluid}$	$f_{O_2}^{fluid} = (X_{CO_2}^{fluid}\gamma_{CO_2}/[K_1X_{CO}^{fluid}\gamma_{CO}])^2$ $a_C^{fluid} = P\,X_{CO_2}^{fluid}\gamma_{CO_2}/(K_2\,f_{O_2}^{fluid})$ $X_{CO}^{fluid} = 1 - X_{CO_2}^{fluid}$

See Table 1 for explanation of symbols.

between ~FMQ + 0.2 and ~FMQ − 1.5 depending on the granulite facies P–T conditions (Fig. 7a).

4. Retrograde metamorphism

Generally, granulites show a decompression-cooling retrograde P–T path (e.g., Touret and Huizenga, 2012). Most retrograde minerals comprise H_2O, suggesting that aqueous retrograde fluids were present during cooling. On the other hand, numerous granulite terrains show that retrograde fluid inclusions have a similar CO_2-rich composition (but different density) as the peak metamorphic inclusions (Touret and Huizenga, 2011). This indicates that retrograde metamorphism occurred in an H_2O-absent environment. It is likely that H_2O-rich fluids can only exist for a relatively short time during retrograde

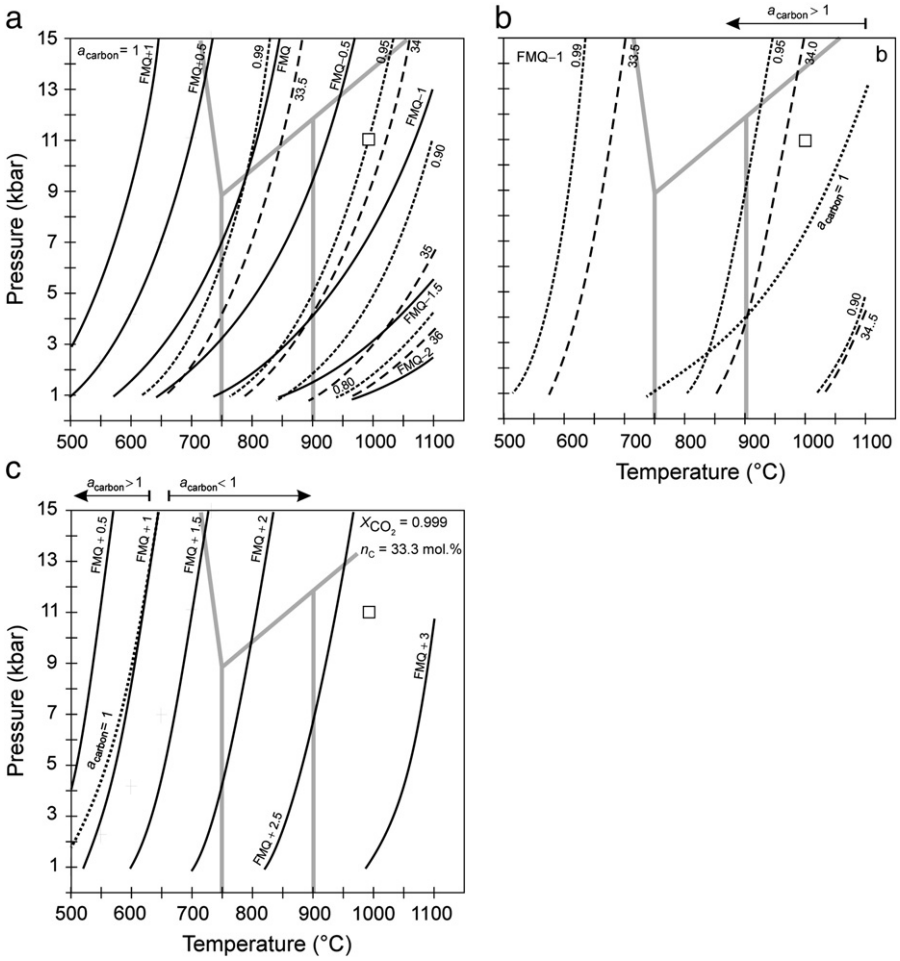

Fig. 7. Calculation results for C–O fluid systems for three different scenarios listed in Table 2. (a) Pressure–temperature diagram showing $f_{O_2}^{fluid}$ (solid black lines, labelled in $\log_{10}$ values relative to FMQ), isopleths of the CO_2 mole fraction ($X_{CO_2}^{fluid}$, fine dashed lines), and the fluid carbon content (n_C, coarse dashed lines, labelled in mol%) for a carbon-saturated C–O fluid system. Open square (P = 11 kbar, T = 1000 °C): carbon-saturated C–O fluid of which $\log_{10} f_{O_2}^{fluid}$ = FMQ − 0.78, $X_{CO_2}^{fluid}$ = 0.95, and n_C = 33.9 mol%. (b) Calculation results of a_C^{fluid} (dotted line, a_C^{fluid} = 1), $X_{CO_2}^{fluid}$ (fine dashed lines), and the fluid carbon content (coarse dashed lines, labelled in mol%) for a C–O fluid of which $\log_{10} f_{O_2}^{fluid}$ is fixed at FMQ − 1. Dotted line separates fluids with $a_C^{fluid} > 1$ (low T) and $a_C^{fluid} < 1$ (high T). Open square (P = 11 kbar, T = 1000 °C): carbon-supersaturated C–O fluid of which a_C^{fluid} = 1.6, $X_{CO_2}^{fluid}$ = 0.93, and n_C = 34.1 mol%. (c) Calculation results of a_C^{fluid} (dotted line, a_C^{fluid} = 1) and $\log_{10} f_{O_2}^{fluid}$ (grey lines) for a C–O fluid of which $X_{CO_2}^{fluid}$ = 0.999. Open square (P = 11 kbar, T = 1000 °C): carbon undersaturated fluid (a_C^{fluid} = 0.0003) of which $X_{CO_2}^{fluid}$ = 0.999 and $\log_{10} f_{O_2}^{fluid}$ = FMQ + 2.7. Dotted line separates C–O fluids with $a_C^{fluid} > 1$ (low T) and $a_C^{fluid} < 1$ (high T). Granulite subfacies indicated in (a), (b), and (c) are after Brown (2007) (see Fig. 2d for field definitions).

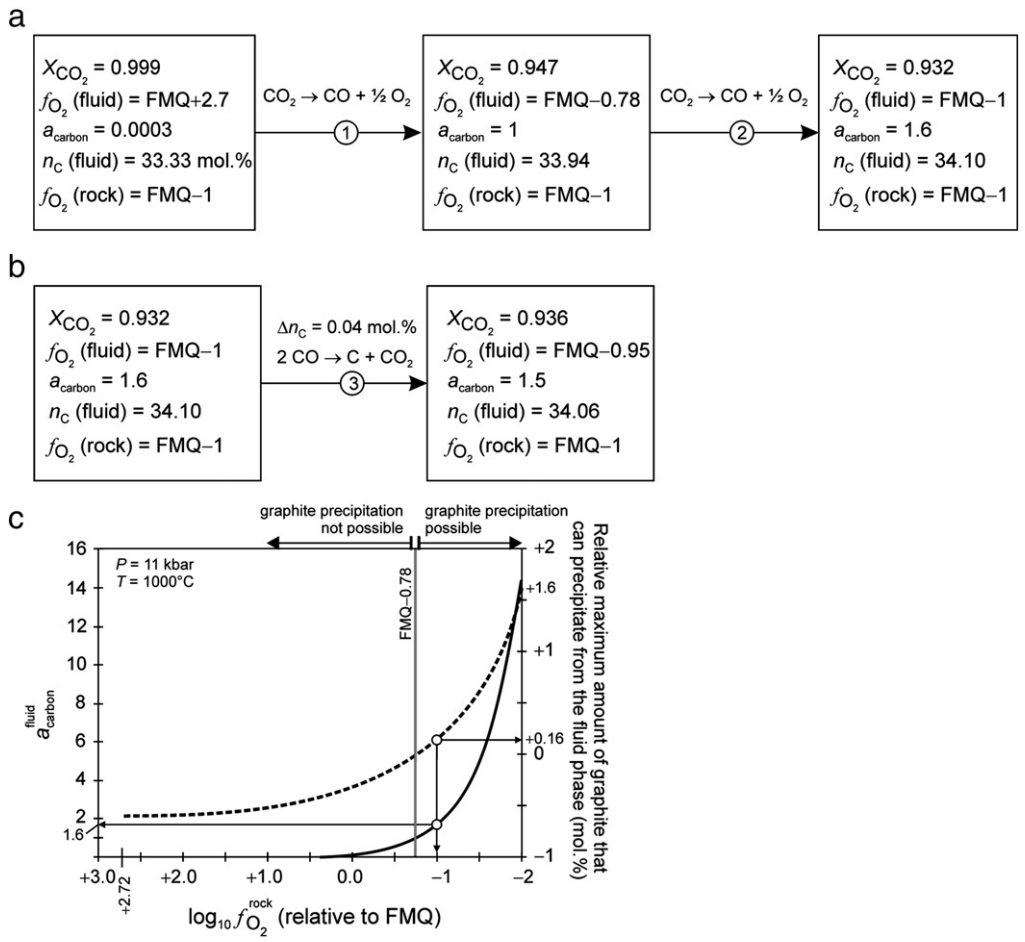

Fig. 8. (a) Chemical evolution of an oxidised CO_2 carbon-undersaturated ($\log_{10} f^{fluid}_{O_2}$ = FMQ + 2.7, a^{fluid}_C = 0.0003, see Fig. 7c) fluid that infiltrates a dry granulite ($\log_{10} f^{rock}_{O_2}$ = FMQ − 1) at P = 11 kbar and T = 1000 °C. Reduction of CO_2 causes the fluid to reach carbon saturation at $\log_{10} f^{fluid}_{O_2}$ = FMQ − 0.78 (see Fig. 7a). The fluid becomes carbon supersaturated if reduction of CO_2 continues until fluid–rock redox equilibrium is reached ($\log_{10} f^{fluid}_{O_2} = \log_{10} f^{rock}_{O_2}$ = FMQ − 1, a^{fluid}_C = 1.6, see Fig. 7b). (b) Graphite precipitation is only possible if fluid–rock redox disequilibrium ($f^{fluid}_{O_2} > f^{rock}_{O_2}$) is possible. The difference between $f^{fluid}_{O_2}$ and $f^{rock}_{O_2}$ is arbitrarily set at + 0.05 $\log_{10}$ units. See text for further discussion. (c) Variation of a^{fluid}_C (solid line) and the maximum amount of graphite that can precipitate (dashed line) as a function of $f^{rock}_{O_2}$. The diagram illustrates that if $\log_{10} f^{rock}_{O_2}$ > FMQ − 0.78, a^{fluid}_C will be < 1 and the maximum amount of graphite that can precipitate is negative, i.e. a CO_2 fluid that infiltrates into a dry granulite which has $\log_{10} f^{rock}_{O_2}$ > FMQ − 0.78 cannot precipitate graphite. Open circles: CO_2 that infiltrates a dry granulite with $\log_{10} f^{rock}_{O_2}$ = FMQ − 1 may result in graphite precipitation (a^{fluid}_C = 1.6) up to a maximum 0.16 mol%. See text for further explanation.

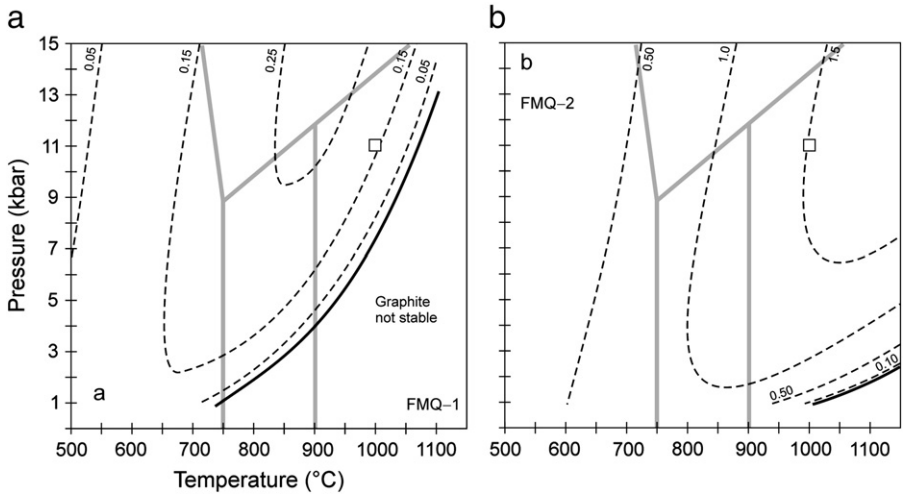

Fig. 9. Maximum relative amount of graphite (Δn_C, dashed lines, labelled in mol.%) that can precipitate upon CO_2 infiltrating a dry rock with a redox state of (a) $\log_{10} f^{rock}_{O_2}$ = FMQ − 1, and (b) $\log_{10} f^{rock}_{O_2}$ = FMQ − 2. Infiltration of CO_2 at P–T conditions of 11 kbar, 1100 °C, respectively, and $\log_{10} f^{rock}_{O_2}$ = FMQ − 1 may result in up to ~0.16 mol% of the carbon in the fluid phase to precipitate as graphite (open square in a). This amount increases to ~1.6 mol% for a more reduced rock ($\log_{10} f^{rock}_{O_2}$ = FMQ − 2) (open square in b). Granulite subfacies indicated in (a) and (b) are after Brown (2007) (see Fig. 2d for field definitions).

metamorphism as H_2O is consumed by hydration reactions (Yardley, 1997, 2009). Alternatively, an H_2O-rich fluid may exist as an equilibrium phase if the rock has already been extensively hydrated (Yardley, 2009). In the next sections, we consider the effect that cooling and decompression have on both C–O–H (H_2O-present) and C–O (H_2O-absent) fluid systems with respect to their graphite precipitation and graphite consumption capabilities.

4.1. Retrograde metamorphism: C–O–H fluid system

The atomic carbon content of a carbon-saturated C–O–H fluid depends on the *P*, *T* and $f_{O_2}^{fluid}$ (e.g., Luque et al., 1998) (Fig. 10a–e). Cooling and decompression of the fluid, while $f_{O_2}^{fluid}$ is buffered by the host-rock, may result in graphite consumption or precipitation as the fluid carbon content increases or decreases, respectively. This can be evaluated by calculating the isopleths for the fluid atomic carbon content for the graphite–C–O–H fluid system for different f_{O_2} conditions (Fig. 10a–d) (e.g., Pasteris, 1999; Huizenga, 2011). Graphite precipitation at $T<\sim600$°C (according to the net reaction 2) is expected from a C–O–H fluid that is subjected to retrograde metamorphism when the fluid–rock system has $\log_{10} f_{O_2} >$ FMQ (Fig. 10a,b). For more reduced fluid–rock systems, the temperature range at which graphite precipitation occurs during retrograde metamorphism shifts to higher temperatures (Fig. 10c–d).

Graphite consumption is expected to occur during retrograde metamorphism at relatively high temperatures ($T<850$ °C) for relatively reduced fluid–rock systems (e.g., at $T<\sim850$°C if $\log_{10} f_{O_2} =$ FMQ − 2, Fig. 10d), whereas for more oxidised systems graphite consumption occurs at lower temperatures (Fig. 10b,c). Whether graphite will be partially or completely consumed cannot be predicted from the thermodynamic calculations and depends on the fluid–graphite ratio. The net graphite consumption reaction involves graphite reacting with H_2O according to the reaction $C + 2\ H_2O \rightarrow CH_4 + O_2$, where O_2 is absorbed by the host–rock (Huizenga, 2011).

It is interesting to note that for fluid–rock systems with $\log_{10} f_{O_2} >$ FMQ, graphite precipitation caused by CO_2 infiltration at granulite facies *P–T* conditions is unlikely as f_{O_2} is too high for graphite to coexist with a C–O–H fluid. However, it is for these redox

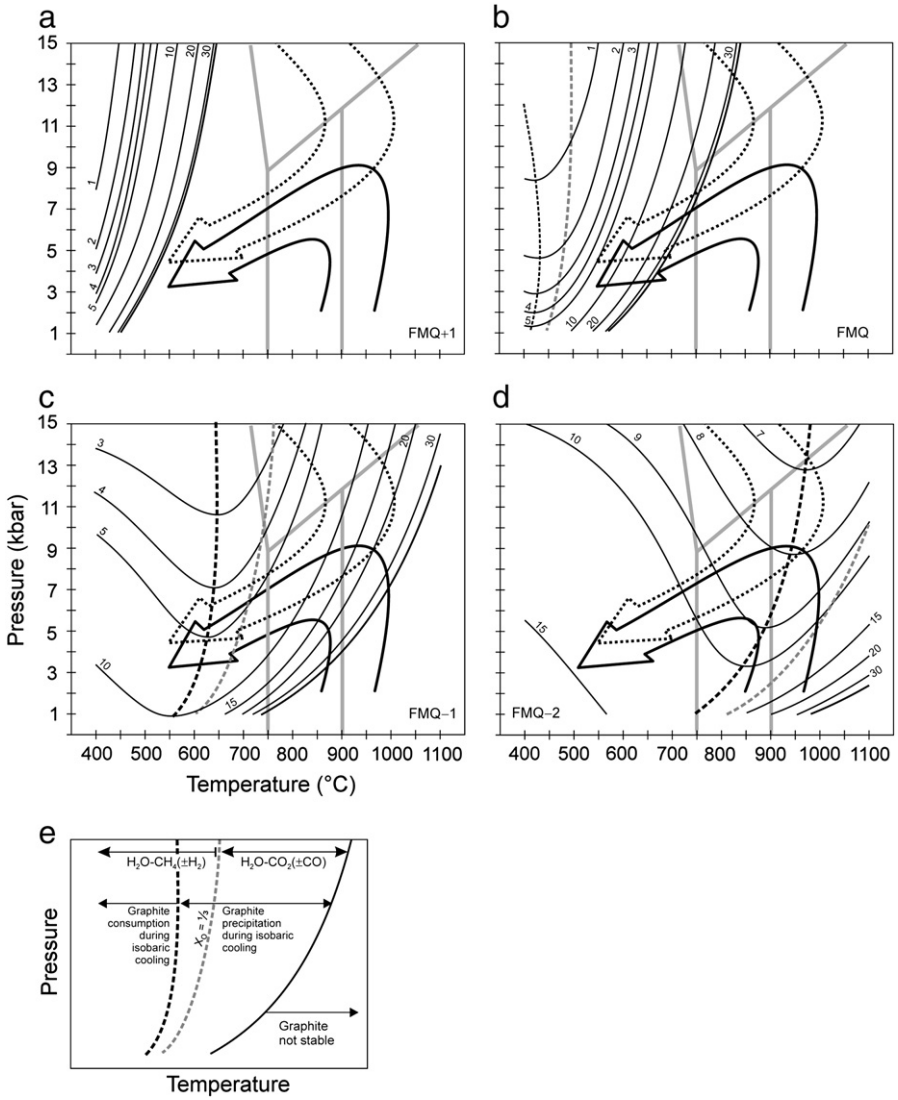

Fig. 10. Atomic carbon isopleths (n_C, thin solid lines, labelled in mol.%) for a carbon-saturated C–O–H fluid for different oxygen fugacities: (a) $\log_{10} f_{O_2}^{fluid} =$ FMQ − 2 (b), $\log_{10} f_{O_2}^{fluid} =$ FMQ − 1 (c), $\log_{10} f_{O_2}^{fluid} =$ FMQ (d), $\log_{10} f_{O_2}^{fluid} =$ FMQ + 1 (modified after Huizenga, 2011). The explanation of the different fields in diagrams (a)–(d) is shown in (e). If n_C decreases during retrograde metamorphism, graphite precipitation will occur whereas if n_C increases graphite consumption will occur. *P–T* fields of graphite precipitation (atomic carbon isopleths have a positive slope) and graphite consumption (atomic carbon isopleths have a negative slope) during isobaric cooling are separated from each other by the black dashed line. High-pressure (dotted arrow) and (ultra)high temperature (solid arrow) granulite *P–T* paths are indicated (Touret and Huizenga, 2012). Grey dashed line: fluids of which $X_O = ⅓$. Fluids with $X_O < ⅓$ (low *T*) comprise $H_2O - CH_4$ ($\pm H_2$), fluids with $X_O > ⅓$ (high *T*) consist of $H_2O - CO_2$ ($\pm$CO). Granulite subfacies indicated in (a)–(d) are after Brown (2007) (see Fig. 2d for field definitions).

conditions that graphite precipitation from a C–O–H fluid can be expected during retrograde metamorphism. On the other hand, for fluid–rock systems with $\log_{10} f_{O_2}$<FMQ, graphite precipitation caused by CO_2 infiltration at granulite facies *P–T* conditions is likely, but there is a distinct possibility that this graphite may be (partially) consumed by a C–O–H fluid during retrograde metamorphism.

4.2. Retrograde metamorphism: C–O fluid system

The atomic carbon content for carbon-saturated C–O fluids shows a consistent decrease with decreasing *T* whereas both $f_{O_2}^{fluid}$ (relative to FMQ) and $X_{CO_2}^{fluid}$ are increasing (Fig. 7a). These changes can be attributed to the precipitation of graphite according to reaction 4. Similar to graphite precipitation from C-O fluids at isobaric-isothermal conditions, graphite precipitation during retrograde metamorphism is only possible if $f_{O_2}^{fluid}$ is not buffered by the rock system ($f_{O_2}^{fluid} \neq f_{O_2}^{rock}$). In that case, the maximum relative amount of graphite that can precipitate will be very small (Fig. 7a). Graphite consumption by a C-O fluid (according to the reverse of reaction 4) is only possible if retrograde metamorphism is near isothermal decompression in which case both $f_{O_2}^{fluid}$ (relative to FMQ) and $X_{CO_2}^{fluid}$ will decrease (Fig. 7a). Again, this is only possible if $f_{O_2}^{fluid}$ is not buffered by the rock system.

5. Discussion and conclusions

The presence or absence of graphite in granulites has been used as evidence either to support or to oppose CO_2 infiltration into lower crustal rocks (Glassley, 1982, Lamb and Valley, 1984, 1985; Santosh and Omori, 2008). We have demonstrated that numerous factors control whether graphite precipitates upon CO_2 infiltration into granulites. Overall, this study has shown that the interpretation of the presence or absence of graphite in granulites in relation to CO_2 infiltration is complicated and requires information on the presence of H_2O and *P–T–*$f_{O_2}^{rock}$ conditions during peak and retrograde metamorphism. The most important conclusions of this study are the following:

(1) For both C–O–H and C–O fluid systems, graphite cannot precipitate upon CO_2 infiltration in rocks when the oxidation state is too high for graphite to coexist with a fluid phase.
(2) Depending on the *P–T–*$f_{O_2}^{rock}$ conditions, graphite precipitation as a result of CO_2 infiltration into a C–O–H fluid-bearing granulite can be considerable. No graphite will precipitate upon CO_2 infiltration into a dry granulite (C-O fluid system) if fluid–rock redox equilibrium is maintained. However, precipitation of small amounts of graphite is possible if $f_{O_2}^{fluid}$ can increase relative to $f_{O_2}^{rock}$.
(3) Graphite precipitation is only possible if the host-rock can absorb the oxygen that is released from the relevant reactions that occur in the fluid phase (reactions 1, 2 and 3). This depends on the ability of the host-rock to absorb O_2 efficiently while maintaining a constant $f_{O_2}^{rock}$ (i.e., buffering capacity, Lamb and Valley, 1984, 1985). The capacity of the host-rock to act as an unlimited oxygen sink is thus critically important for graphite precipitation to take place. The fluid becomes an oxidising agent for the host-rock if it does not have the capacity to absorb the oxygen while keeping $f_{O_2}^{rock}$ fixed at its buffer value, a scenario that is likely when the CO_2 fluid–rock ratio is large. In that case, CO_2 may become an oxidising agent for the host-rock. Host-rock oxidation by CO_2 may be an explanation of the high oxidation state observed in numerous (graphite-absent) granulite terrains (e.g., Newton and Manning, 2005; Newton, 2011), including the Archean Shevaroy Hills in Southern India (Harlov et al., 1997) and Pan African granulites of the Furua Complex in Tanzania (Coolen, 1980). The high $f_{O_2}^{rock}$ can, however, also explained by a relative high intrinsic $f_{O_2}^{rock}$ (not allowing graphite to precipitate when CO_2 infiltration occurred as $f_{O_2}^{rock}$ is too high for graphite to be stable), or the infiltration of oxidised (sulphate-bearing) brine solutions (Harlov et al., 1997; Newton and Manning, 2005).
(4) During retrograde metamorphism graphite can either precipitate or be consumed when a C–O–H fluid is present. Relatively reduced C–O–H fluids ($\log_{10} f_{O_2}$<FMQ) show generally an increase of the carbon solubility with decreasing *T*, i.e., the fluid may dissolve graphite during retrograde metamorphism. A more oxidised C–O–H fluid ($\log_{10} f_{O_2}$>FMQ), on the other hand, may precipitate significant amounts of graphite due to the decrease of the carbon solubility with decreasing *T*. The amount of graphite that can precipitate from a C–O fluid during retrograde metamorphism in an H_2O-absent environment is insignificantly small.

Acknowledgements

Comments on an earlier version of this paper by Bernardo Cesare and Doug Rumble are highly appreciated. Bernardo Cesare is also thanked for allowing us to use his photograph (Fig. 1). We would like to thank HM Rajesh and an anonymous reviewer for their constructive reviews, and M. Santosh for his editorial support. This work was supported through funding by the National Research Foundation of South Africa to J.M. Huizenga.

References

Andreae, M.O., 1974. Chemical and stable isotope composition of the high grade metamorphic rocks from the Arendal area, Southern Norway. Contributions to Mineralogy and Petrology 47, 299–316.
Berg, J.H., 1977. Dry granulite mineral assemblages in the contact aureoles of the Nain Complex, Labrador. Contributions to Mineralogy and Petrology 64, 33–52.
Berglund, L., Touret, J., 1976. Garnet–biotite gneiss in 'Système du Graphite' (Madagascar): petrology and fluid inclusions. Lithos 9, 139–148.
Binu-Lal, S.S., Kehelpannalab, W., Satish-Kumar, M., Wada, H., 2003. Multistage graphite precipitation through protracted fluid flow in sheared metagranitoid, Digana, Sri Lanka: evidence from stable isotopes. Chemical Geology 197, 253–270.
Bohlen, S.R., Essene, E.J., 1977. Feldspar and oxide thermometry of granulites in the Adirondack Highlands. Contributions to Mineralogy and Petrology 62, 153–169.
Brown, M., 2007. Metamorphism, plate tectonics, and the supercontinent cycle. Earth Science Frontiers 14, 1–18.
Cesare, B., Maineri, C., 1999. Fluid-present anatexis of metapelites at El Joyazo (SE Spain): constraints from Raman spectroscopy of graphite. Contributions to Mineralogy and Petrology 135, 41–52.
Cesare, B., Meli, S., Nodari, L., Russo, U., 2005. Fe^{3+} reduction during biotite melting in graphitic metapelites: another origin of CO_2 in granulites. Contributions to Mineralogy and Petrology 149, 129–140.
Collins, A.S., Kinny, P.D., Razakamanana, T., 2012. Depositional age, provenance and metamorphic age of metasedimentary rocks from southern Madagascar. Gondwana Research 21, 353–361.
Coolen, J.J.M.M.M., 1980. Chemical petrology of the Furua Granulite Complex, Southern Tanzania: GUA Papers of Geology, University of Amsterdam, Series, 1, p. 258.
Crespo, E., Luque, J., Fernández-Rodríguez, C., Rodas, M., Díaz-Azpiroz, M., Fernández-Caliani, J.C., Barrenechea, J.F., 2004. Significance of graphite occurrences in the Aracena Metamorphic Belt, Iberian Massif. Geological Magazine 141, 687–697.
Dunai, T.J., Touret, J.L.R., 1993. A noble gas study of a granulite sample from the Nilgiri Hills, southern India: implications for granulite formation. Earth and Planetary Science Letters 119, 271–281.
Farquhar, J., Chacko, T., 1991. Isotopic evidence for involvement of CO_2-bearing magmas in granulite formation. Nature 354, 60–63.
Farquhar, J., Hauri, E., Wang, J., 1999. New insights into carbon fluid chemistry and graphite precipitation: SIMS analysis of granulite facies graphite from Ponmudi, South India. Earth and Planetary Science Letters 171, 607–621.
French, B.M., 1966. Some geological implications of equilibrium between graphite and a C–O–H gas at high temperatures and pressures. Reviews of Geophysics 4, 223–253.
Fyfe, W.S., 1973. The granulite facies, partial melting and the Archean crust. Philosophical Transactions of the Royal Society of London A273, 457–461.
Glassley, W., 1982. Fluid evolution and graphite genesis in the deep continental crust. Nature 295, 229–231.
Hacker, B.R., Gnos, E., Ratschbacher, L., Grove, M., McWilliams, M., Sobolev, S.V., Wan, J., Zhendan, W., 2000. Hot and dry deep crustal xenoliths from Tibet. Science 287, 2463–2466.
Harley, S.L., 2004. Extending our understanding of ultrahigh temperature crustal metamorphism. Journal of Mineralogical and Petrological Sciences 99, 140–158.
Harlov, D.E., 1992. Comparative oxygen barometry in granulites, Bamble Sector, SE Norway. Journal of Geology 100, 447–464.
Harlov, D.E., 2000. Titaniferous magnetite ± ilmenite thermometry and titaniferous magnetite ± ilmenite ± orthopyroxene ± quartz oxygen barometry in granulite

facies gneisses, Bamble Sector, SE Norway: implications for the role of high-grade CO_2-rich fluids during granulite genesis. Contributions to Mineralogy and Petrology 139, 180–197.
Harlov, D.E., Newton, R.C., Hansen, E.C., Janardhan, A.S., 1997. Oxide and sulphide minerals in highly oxidized, Rb-depleted, Archaean granulites of the Shevaroy Hills Massif, South India: oxidation states and the role of metamorphic fluids. Journal of Metamorphic Geology 15, 701–717.
Holland, T.J.B., Powell, R., 1998. An internally consistent thermodynamic data set for phases of petrological interest. Journal of Metamorphic Geology 16, 309–343.
Hollister, L.S., 1988. On the origin of CO_2-rich fluid inclusions in migmatites. Journal of Metamorphic Geology 6, 467–474.
Huizenga, J.M., 2001. Thermodynamic modelling of C – O – H fluids. Lithos 55, 101–114.
Huizenga, J.M., 2005. COH, an Excel spreadsheet for composition calculations in the C – O – H fluid system. Computers & Geosciences 31, 797–800.
Huizenga, J.M., 2011. Thermodynamic modelling of a cooling C – O – H fluid–graphite system: implications for hydrothermal graphite precipitation. Mineralium Deposita 26, 33–43.
Jackson, D.H., Mattey, D.P., Harris, N.B.W., 1988. Carbon isotope compositions of fluid inclusions in charnockites from southern India. Nature 333, 167–170.
Lamb, W., Valley, J.W., 1984. Metamorphism of reduced granulites in low-CO_2 vapour-free environment. Nature 312, 56–58.
Lamb, W., Valley, J.W., 1985. C – O – H fluid calculations and granulite genesis. In: Tobi, A.C., Touret, J.L.R. (Eds.), The Deep Proterozoic Crust in the North Atlantic Provinces. NATO Science Series: C: Mathematical & Physical Sciences, Vol. 158. Reidel, Dordrecht, pp. 119–139.
Luque, F.J., Pasteris, J.D., Wopenka, B., Rodas, M., Barrenecha, J.F., 1998. Natural fluid-deposited graphite: mineralogical characteristics and mechanisms of formation. American Journal of Science 298, 471–498.
Luque, F.J., Crespo-Feo, E., Barrenechea, J.F., Ortega, L., 2012. Carbon isotopes of graphite: implications on fluid history. Geoscience Frontiers 3, 197–207.
Nasipuri, P., Bhattacharya, A., Das, S., 2009. Metamorphic reactions in dry and aluminous granulites: a Perple_X P–T pseudosection analysis of the influence of effective reaction volume. Contributions to Mineralogy and Petrology 157, 301–311.
Newton, R.C., 2011. Three partners of metamorphic petrology. American Mineralogist 96, 457–469.
Newton, R.C., Manning, C.E., 2005. Solubility of anhydrite, $CaSO_4$, in $NaCl - H_2O$ solutions at high pressure and temperatures: applications to fluid–rock interaction. Journal of Petrology 46, 701–716.
Newton, R.C., Smith, J.C., Windley, B.F., 1980. Carbonic metamorphism, granulites and crustal growth. Nature 288, 45–50.
Newton, R.C., Aranovich, L.Ya., Hansen, E.C., Vandenheuvel, B.A., 1998. Hypersaline fluids in Precambrian deep-crustal metamorphism. Precambrian Research 91, 41–63.
Nockleberg, W.J., 1973. CO_2 as a source of oxygen in the metasomatism of carbonates. American Journal of Science 273, 498–514.
Ohmoto, H., Kerrick, D., 1977. Devolatilization equilibria in graphitic systems. American Journal of Science 277, 1013–1044.
Pasteris, J.D., 1999. Causes of uniformly high crystallinity of graphite in large epigenetic deposits. Journal of Metamorphic Geology 17, 779–787.
Perry, E.C., Ahmad, S.N., 1977. Carbon isotope composition of graphite and carbonate minerals from 3.8-AE metamorphosed sediments, Isuakasia, Greenland. Earth and Planetary Science Letters 36, 280–284.
Pili, E., Sheppard, S.M.F., Lardeaux, J.-M., 1998. Fluid-rock interaction in the granulites of Madagascar and lithospheric-scale transfer of fluids. Gondwana Research 2, 341–350.
Radhika, U.P., Santosh, M., 1996. Shear-zone hosted graphite in southern Kerala, India: implications for CO_2 infiltration. Journal of Asian Earth Sciences 14, 265–273.
Rodas, M., Luque, J., Barrenechea, J.F., Fernández-Caliani, J.C., Miras, A., Fernández-Rodríguez, C., 2000. Graphite occurrences in the low-pressure/high-temperature metamorphic belt of the Sierra de Aracena (southern Iberian Massif). Mineralogical Magazine 64, 801–814.
Rumble, D., Hoering, T.L., Grew, E.S., 1977. The relation of carbon isotopic composition to graphitization of carbonaceous materials from the Narragansett Basin, Rhode Island: Carnegie Institution of Washington Year Book, 76, pp. 623–625.
Rumble, D., Duke, E.F., Hoering, T.L., 1986. Hydrothermal graphite in New Hampshire: evidence of carbon mobility during regional metamorphism. Geology 14, 452–455.
Sajeev, K., Osanai, Y., Connolly, J.A.D., Susuki, S., Ishioka, J., Kagami, H., Rino, S., 2007. Extreme crustal metamorphism during a Neoproterozoic event in Sri Lanka: a study of dry mafic granulites. Journal of Geology 115, 563–582.
Santosh, M., Omori, S., 2008. CO_2 flushing: a plate tectonic perspective. Gondwana Research 13, 86–102.
Santosh, M., Wada, H., 1993a. A carbon isotope study of graphites from the Kerala Khondalite Belt, Southern India: evidence for CO_2 infiltration in granulites. Journal of Geology 101, 643–651.
Santosh, M., Wada, H., 1993b. Microscale isotopic zonation in graphite crystals: evidence for channelled CO_2 influx in granulites. Earth and Planetary Science Letters 119, 19–26.
Santosh, M., Harris, N.B.W., Jackson, D.H., Mattey, D.P., 1990. Dehydration and incipient charnockite formation: a phase equilibria and fluid inclusion study from South India. Journal of Geology 98, 915–926.
Santosh, M., Wada, H., Satish-Kumar, M., Binu-Lal, S.S., 2003. Carbon isotope "stratigraphy" in a single graphite crystal: implications for the crystal growth mechanism of fluid-deposited graphite. American Mineralogist 88, 1689–1696.
Santosh, M., Tsunogae, T., Yoshikura, S., 2004. "Ultrahigh density" carbonic fluids in ultrahigh-temperature crustal metamorphism. Journal of Mineralogical and Petrological Sciences 99, 164–179.
Santosh, M., Tsunogae, T., Ohyama, H., Sato, K., Li, J.H., Liu, S.J., 2008. Carbonic metamorphism at ultrahigh-temperatures: evidence from North China Craton. Earth and Planetary Science Letters 266, 149–165.
Satish-Kumar, M., Yurimoto, H., Itoh, S., Cesare, B., 2011. Carbon isotope anatomy of a single graphite crystal in a metapelitic migmatite revealed by high-spatial resolution SIMS analysis. Contributions to Mineralogy and Petrology 162, 821–834.
Shi, P., Saxena, S.K., 1992. Thermodynamic modelling of the C – O – H – S fluid system. American Minarologist 77, 1038–1049.
Skippen, G.B., Marshall, D.D., 1991. The metamorphism of granulites and devolitalization of the lithosphere. The Canadian Mineralogist 29, 693–705.
Török, K., Dégi, J., Szép, A., Marosi, G., 2005. Reduced carbonic fluids in mafic granulite xenoliths from the Bakony-Balaton Highland Volcanic Field, W-Hungary. Chemical Geology 223, 93–108.
Touret, J.L.R., 1971. Le faciès granulite en Norvège méridionale. II Les inclusions fluides. Lithos 4, 423–436.
Touret, J.L.R., 1992. CO_2 transfer between the upper mantle and the atmosphere: temporary storage in the lower continental crust. Terra Nova 4, 87–98.
Touret, J.L.R., Huizenga, J.M., 2011. Fluids in granulites. In: van Reenen, D.D., Kramers, J.D., McCourt, S., Perchuk, L.L. (Eds.), Origin and evolution of Precambrian high-grade gneiss terranes, with special emphasis on the Limpopo Complex of Southern Africa: Geological Society of America Memoir, 207, pp. 25–37.
Touret, J.L.R., Huizenga, J.M., 2012. Fluid-assisted granulite metamorphism: a continental journey. Gondwana Research 21, 224–235.
Touret, J.L.R., Nijland, T.G., 2012. Prograde, peak and retrograde metamorphic fluids and associated metasomatism in upper amphibolite to granulite facies transition zones. In: Harlov, D., Austrheim, H. (Eds.), Metasomatism and chemical transformation of rock. The role of fluids in terrestrial and extraterrestrial processes. Lecture Notes in Earth System Sciences. Springer, Berlin.
Tsunogae, T., Santosh, M., Osanai, Y., Owada, M., Toyoshima, T., Hokada, T., 2002. Very high-density carbonic fluid inclusions in sapphirine-bearing granulites from Tonagh Island in the Archean Napier Complex, East Antarctica: implications for CO_2 infiltration during ultrahigh-temperature ($T > 1100°C$) metamorphism. Contributions to Mineralogy and Petrology 143, 279–299.
Wada, H., Tomita, T., Matsuura, K., Iuchi, K., Ito, M., Morikiyo, T., 1995. Graphitization of carbonaceous matter during metamorphism with references to carbonate and pelitic rocks of contact and regional metamorphism, Japan. Contributions to Mineralogy and Petrology 118, 217–228.
Watson, E.B., Brenan, J.M., 1987. Fluids in the lithosphere, 1 Experimentally determined wetting characteristics of $CO_2 - H_2O$ fluids, their implications for fluid transport, host-rock physical properties, and fluid inclusion formation. Earth and Planetary Science Letters 85, 497–515.
Yardley, B.W.D., 1997. The evolution of fluids through the metamorphic cycle. In: Jamtveit, B., Yardley, B.W.D. (Eds.), Fluid Flow and Transport in Rocks. Chapman & Hill, London, pp. 99–121.
Yardley, B.W.D., 2009. The role of water in the evolution of the continental crust. Journal of the Geological Society of London 166, 585–600.
Zhang, C., Duan, Z., 2010. GFluid: an Excel spreadsheet for investigating C – O – H fluid composition under high temperatures and pressures. Computers & Geosciences 36, 569–572.
Zhang, Z., Shen, K., Santosh, M., Dong, X., 2011. High density carbonic fluids in a slab window: evidence from the Gangdese charnockites, Lhasa terrane, southern Tibet. Journal of Asian Earth Sciences 42, 515–524.